Energies of the Anharmonic Oscillator using the Metropolis Algorithm and Matrix Methods

B A Ngwenya[1], A K Rothkopf[2] and W A Horowitz[1]

[1]Department of Physics, University of Cape Town, Rondebosch 7700, South Africa

[2]Department of Mathematics and Physics, University of Stavanger, PO Box 8600, 4036 Stavanger, Norway

E-mail: ngwble001@myuct.ac.za

Abstract. We present results of the energies and energy differences of the quantum harmonic oscillator as well as the quantum anharmonic oscillator at quartic coupling constants of different magnitudes. These observables are computed using the Markov Chain Monte Carlo approach (Metropolis Algorithm) and are compared to results obtained using matrix elements methods at various basis sizes. We illustrate the consistency in the two methods and show that for the anharmonic oscillator, a sufficiently large basis size is required with increasing energy in order for the matrix result to converge to the lattice result. We also show that large quartic coupling constants are more sensitive to the truncation of the basis size.

1. Introduction

In classical mechanics, the harmonic oscillator is a very popular example of a restoring force acting on an object about its equilibrium position, and has many applications. In a one dimensional case, one can consider a particle of mass, m, attached to a spring and experiencing a restoring force as described by Hooke's law [1], $F = -kx$. The corresponding potential energy is given by $E = kx^2/2$, has a parabolic shape and describes the continuous energies that the particle can attain during its oscillation. The quantum harmonic oscillator is the corresponding analogue of the harmonic oscillator in quantum mechanics and is characterized by the Schrodinger equation [2],

$$\hat{H}\psi = \left(-\frac{\hbar^2}{2m}\frac{d^2}{dx^2} + \frac{m\omega^2 x^2}{2}\right)\psi = E\psi \tag{1}$$

where the first term in the Hamiltonian ($\hat{H}$) is the kinetic term and the second term is the same potential we saw in the classical analogue, with $\omega = \sqrt{k/m}$ and describes the natural frequency of the oscillator. Various analytical methods have been formulated to solve the above equation for the energy eigenvalues, and they show that unlike in the classical case, the energies of the quantum harmonic oscillator are discrete, quantized and given by [3];

$$E_n = \left(n + \frac{1}{2}\right)\hbar\omega \tag{2}$$

where $n = 0$ corresponds to the ground state. Note that this ground state energy is not equal to zero, a consequence of the uncertainty principle [4].

In general, molecular vibrations with arbitrary potentials can be approximated as harmonic potentials around a stable equilibrium through expanding the potential as a Taylor series. The harmonic oscillator describes such an expansion truncated at second order [5]. At higher order, the potential contains quartic terms and the motion becomes that of an anharmonic oscillator. The corresponding Hamiltonian with a quartic term, in one dimension is given by [6],

$$\hat{H} = -\frac{\hbar^2}{2m}\frac{d^2}{dx^2} + \frac{m\omega^2 x^2}{2} + \lambda x^4 \tag{3}$$

where λ is the coupling constant of the quartic (anharmonicity) term.

Unlike the harmonic oscillator which has exact analytic solutions, the anharmonic oscillator cannot be solved analytically and we need to resort to numerical methods. In this paper, we employ the Markov Chain Monte Carlo technique to compute the exact, as well as energy differences of the first few lowest energies of the one-dimensional anharmonic oscillator while varying the coupling constant of the quartic term. We compare these lattice solutions to corresponding results when using matrix elements at varying basis size to explore the effect of basis size truncation on the accuracy of the numerical result.

2. Path Integrals and the Metropolis Algorithm

A starting point in formulating an approach to numerically solve the quantum anharmonic oscillator on the lattice is to build an understanding of how the state of a particle evolves with time. That is, given a particle at (x_0, t_0), what's the probability of finding it at (x_f, t_f), where t_f is some later time. Schrodinger and Heisenberg formulated solutions to this problem employing the eigenstates of the Hamiltonian. As an alternative, Feynman formulated the path integral approach to quantum mechanics [7], motivated by the work of Paul Dirac suggesting that a Lagrangian formulation is more fundamental than a Hamiltonian one.

The main idea behind the path integral formulation is the equivalence of the transition probability amplitude, $< \psi(x_f, t_f)|\psi(x_0, t_0) >$ between any two points and the exponential of the classical action, $\exp\{iS[x(t)]\}$ of the trajectory. Given that a particle cannot take a well-defined path between any two points, Feynman showed that the total transition probability amplitude is given by the sum of the amplitudes of all the possible paths that the particle can take between the two points. We then define the imaginary time propagator (which fully describes the evolution of a system with time) between the two spacetime points as the probability transition amplitude between the wavefunction evaluated at those two points,

$$\begin{aligned} U(x_f, \tau_f; x_0, \tau_0) &= \langle \psi(x_f, \tau_f)|\psi(x_0, \tau_0)\rangle & (4)\\ &= \langle x_f|e^{-\hat{H}(\tau_f - \tau_i)/\hbar}|x_0\rangle & (5)\\ &= \int_{\text{all paths}} \exp\left[-\frac{1}{\hbar}\int_{\tau_i}^{\tau_f} L[x(\tau)]d\tau\right] & (6) \end{aligned}$$

where L is classical Euclidean Lagrangian, and we perform the integration over all possible trajectories between the two spacetime points. Notice also, the Wick rotation (change in the time parameter) $t = -i\tau$, where $\tau = \hbar/k_B T$ is the 'imaginary time' and allows for a direct comparison to the partition function in statistical mechanics. A complete derivation of the above path integral can be found in Ref. [8].

We then use the Metropolis Hastings algorithm [9, 10] to generate the many different paths on the lattice, that can be used to compute the propagator. A discrete time lattice with N_τ sites (lattice points in the time direction), employing periodic boundary conditions (to avoid rejecting paths affected by lattice site edges) is used. Euclidean time increments $\delta\tau$ are used, such that the lattice points are given by $x_i = i\delta\tau$, with $i = 1, ..., N_\tau$. In order to perform these

calculations computationally, we start by expressing our equations in dimensionless form by setting $\hbar = c = 1$ such that the discretised action for the anharmonic oscillator is given by [6],

$$\tilde{S}(\tilde{x}_i) = \sum_{i=1}^{N_\tau} \left[\frac{\tilde{m}}{2}(\tilde{x}_{i+1} - \tilde{x}_i)^2 + \frac{\tilde{m}\tilde{w}^2 \tilde{x}_i{}^2}{2} + \tilde{\lambda}\tilde{m}^2\tilde{w}^3\tilde{x}_i{}^4 \right] \tag{7}$$

$$\tilde{x}_i = \frac{x_i}{\delta\tau}, \quad \tilde{m} = m\delta\tau, \quad \tilde{\omega} = \omega\delta\tau \tag{8}$$

where $\tilde{x}_i$, $\tilde{m}$, $\tilde{\omega}$ and $\tilde{\lambda}$ are dimensionless variables.

The Metropolis algorithm requires as an input an array with N_τ entries containing the initial path between the two points. This initial path can be set to an array of zeros (a cold start), or an array of random numbers (a hot start). We also need to input a real number, h the target interval which determines the acceptance rate in the simulation (i.e. how many paths should be accepted/rejected on average), as well as the various parameters appearing in the action. Every time we traverse through the lattice (one sweep), we produce one trajectory with real coordinates $(x_1, ..., x_{N_\tau})$ in Euclidean time, and these coordinates have probability density $\rho[\{x_i\}] \sim \exp\{-\tilde{S}(\tilde{x}_i)\}$ [11]. This procedure is repeated many times to create an ensamble of paths in Monte Carlo time, forming a Markov Chain and this ensemble of paths is then used for analysis.

Prior to taking any measurements that will be used for analysis, one has to discard the first 'few' paths that are generated before the system thermalises because these paths are not representative of the equilibrium distribution of the system. Given that once the random number generator used to produce these paths is seeded, the produced paths are correlated. To reduce the effect of these correlations in the measurements, one also needs to discard a certain number of paths between any two subsequent measurements used for analysis. These correlations lead to increased uncertainties in the measurements and can be quantified using the autocorrelation time [12].

In Figure 1a, we show the acceptance rate for a step size $\delta\tau = 1$ at various quartic coupling constants. Generally, an acceptance rate of $50 - 60\%$ is sufficient, and if the acceptance rate is too low then most paths will be rejected thus resulting in longer simulation times. A plot of the acceptance rate as a function of the parameter h allows one to pick the a value to achieve the desired acceptance rate. We see that the parameter h is smaller for larger quartic coupling constants. In Figure 1b, we show the thermalisation of $\langle \hat{x}^2 \rangle$ for $\tilde{\lambda} = 1$, $\delta\tau = 1$ starting from a cold start and this can be used to get a sense of the number of paths to discard during thermalisation before taking measurements.

We then make use of these measurements (ensambles of paths) to compute various quantities of interest. The ground state energy is computed from the correlation functions of the position operator $\hat{x}$ [13],

$$E_0 = m\omega^2\langle \hat{x}^2 \rangle + 3\lambda\langle \hat{x}^4 \rangle \tag{9}$$

while the energies are calculated as follows [14, 12];

$$E_1 - E_0 = -\hbar \lim_{\tau\to\infty} \left[\frac{d \log[G_2(\tau)]}{d\tau} \right], \quad G_2(\tau) = \langle \hat{x}(\tau)\hat{x}(0) \rangle - \langle \hat{x}(\tau) \rangle \langle \hat{x}(0) \rangle \tag{10}$$

$$E_2 - E_0 = -\hbar \lim_{\tau\to\infty} \left[\frac{d \log[G_4(\tau)]}{d\tau} \right], \quad G_4(\tau) = \langle \hat{x}(\tau)^2\hat{x}(0)^2 \rangle - \langle \hat{x}(\tau)^2 \rangle \langle \hat{x}(0)^2 \rangle \tag{11}$$

where $G_2(\tau)$ and $G_4(\tau)$ are the connected two-point and four-point correlation functions respectively.

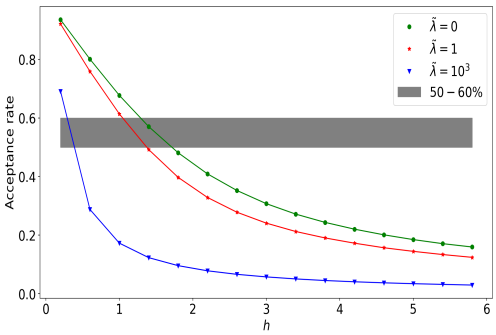

(a) Acceptance rate for $\delta\tau = 1$

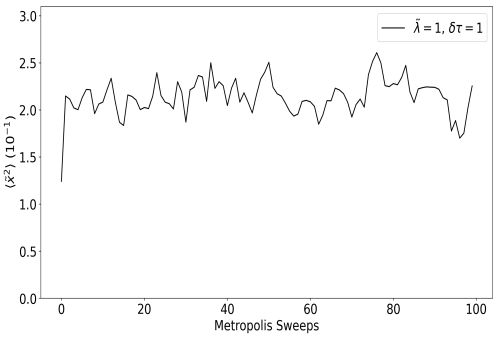

(b) Thermalisation

Figure 1. The acceptance rate as a function of the target interval and the thermalisation of $\langle \hat{x}^2 \rangle$ from a cold start.

3. Results

We start by looking at the oscillator energies, while varying the effective lattice spacing (a). In Figure 1a, we compare ground state energy results of the harmonic oscillator to the known analytical result. The key thing to notice is that MCMC result converges to the analytical result of $E_0 = \frac{1}{2}\hbar\omega$ with decreasing lattice spacing. This is characteristic of lattice calculations which converge to the correct result in the continuum limit (i.e. $a \to 0$). Unfortunately, it's unrealistic to gradually decrease the effective lattice spacing in simulations to it's continuum value as this is limited by computational resources. Instead, one uses the results obtained from a few lattice spacings and extrapolates to the continuum limit. An example of this is shown in Figure 1b where there's no known analytical solutions of the energies of the anharmonic oscillator. In this case, we perform calculations for various lattice spacings, then use cubic splines to extrapolate to the continuum limit and we obtain the result $E_1 - E_0$ from that procedure. The uncertainties are computed using the Jackknife error analysis [15] with a bin size of 10^3.

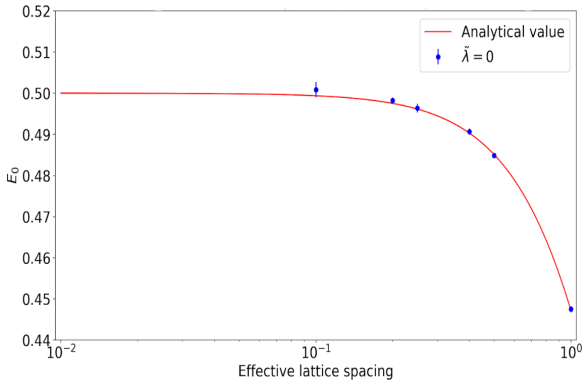

(a) Harmonic oscillator

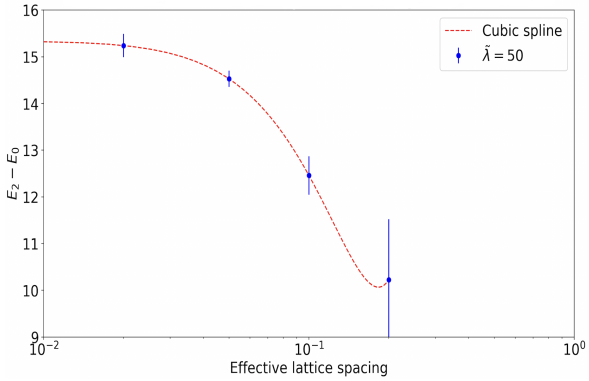

(b) Anharmonic oscillator

Figure 2. Energy of the harmonic and anharmonic oscillator as a function of the effective lattice spacing.

In Figure 3, we show the energies of the ground state and first excited state of the quantum anharmonic oscillator respectively. These energies are computed using matrix elements with varying basis size, and using the correlation functions of the position operator in the lattice

approach. On the lattice, the ground state energy is given by Eq. 9, while the first excited state is obtained from adding E_0 to the two-point connected correlation function in Eq. 10 which gives $E_0 - E_1$. A graphical representation of this energy difference is shown in Figure 4, as well as the energy difference of the second excited state and ground state, which is obtained from the four-point connected correlation function in Eq. 11. In the case of the harmonic oscillator (i.e. $\lambda = 0$), the Hamiltonian matrix is diagonal and we obtain the exact energy eigenvalues for E_0, E_1 etc. irrespective of the basis size (recall that the basis size just gives you the number of energy levels of interest). As we increase the quartic coupling, λ, to a non-zero value (where the Hamiltonian matrix is no longer diagonal) while keeping the basis size the same (i.e. as low as in the harmonic oscillator case), we obtain the correct result for lower energies but inaccurate results for higher energies which are more sensitive to the truncation of the basis size.

The effect of the basis size on the accuracy of the measured energies is also observed as one increases the quartic coupling. In general, the higher the quartic coupling, the more sensitive the energies of the corresponding oscillator are to the truncation of the basis. The reason for this sensitivity is that, the energy values of the various energy levels of the anharmonic oscillator increase with λ i.e. $E_i(\lambda = 0) < E_i(\lambda = 1) < E_i(\lambda = 2)$ etc., where i corresponds to the energy levels. Thus increasing λ implies an increase in the energies, which are sensitive to the truncation of the basis size. Looking at Figure 3 and 4, the effect of the basis truncation is clear at large quartic coupling where the MCMC result is only consistent with the matrix result at a high basis size.

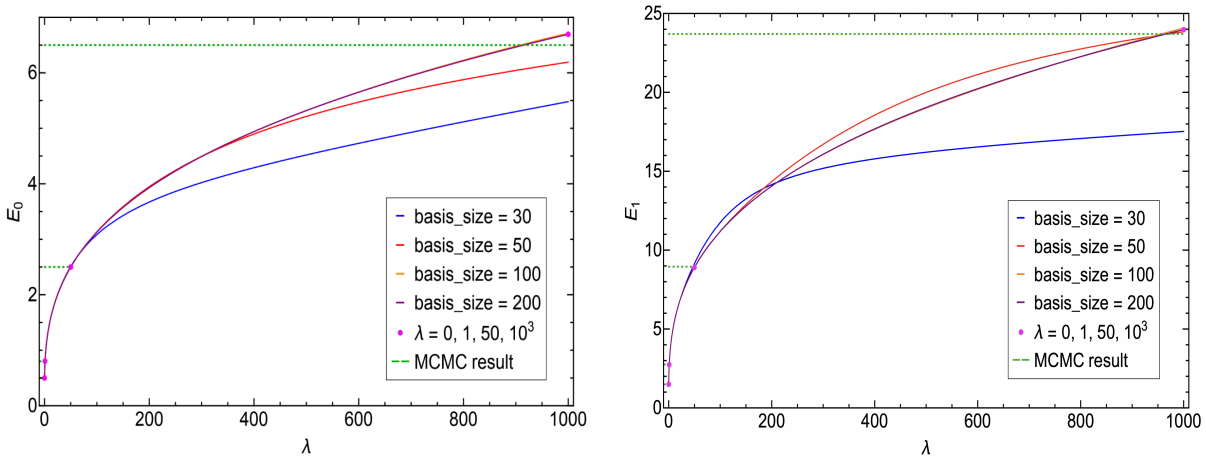

(a) Ground State (b) First Excited State

Figure 3. Comparison of the energies of the harmonic and anharmonic oscillator computed using lattice and matrix methods.

4. Conclusions

We have presented numerical results of the ground state and first two excited states energies of the one-dimensional quantum anharmonic oscillator at varying quartic coupling constants. These energies were computed on the lattice using the metropolis algorithm, which allows for computational solutions to the path integral formulation of quantum mechanics. We compare these lattice results to energy eigenvalues of the Hamiltonian obtained using the matrix elements method for varying basis size.

We showed that one obtains accurate energies for the harmonic oscillator using both the lattice approach and matrix elements even for a small basis size since the Hamiltonian is diagonal. However, for the anharmonic oscillator, higher energies (excited states) are very sensitive to the

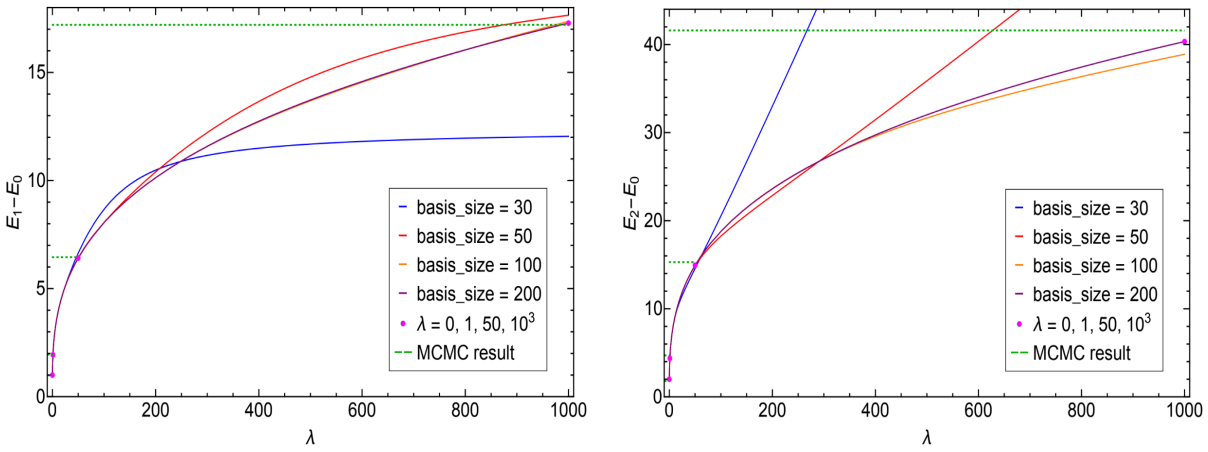

(a) $E_1 - E_0$ (b) $E_2 - E_0$

Figure 4. Harmonic and anharmonic oscillator energy differences computed using lattice and matrix methods.

truncation of the basis size, thus one needs to increase the basis size to improve the accuracy of the numerical result for excited state energies. In addition, we also showed that the larger the quartic coupling constant (λ), the more sensitive the energies are to the basis size truncation. This sensitivity with increasing λ is because the magnitude of the energies at various energy levels increases with increasing λ. At a sufficiently large basis size, we show that the matrix elements result converges to the results obtained on the lattice. While one can compute energies of even higher excited states using matrix elements with a large basis size (limited by computational resources), performing such a calculation on the lattice becomes increasingly difficult due to increasing statistical fluctuations.

Acknowledgments

The authors would like to acknowledge the SA-CERN Collaboration and the South African National Research Foundation (NRF) for their generous financial contributions towards this work.

References

[1] Thompson J O *Science* **64 1656** 298–9
[2] Westbroek M J E, King P R, Vvedensky D D and Dürr S 2018 *Am. J. Phys.* **86** 293 (*Preprint* `1712.08508`)
[3] Griffiths D Introduction to quantum mechanics, 3rd
[4] Busch P, Heinonen T and Lahti P 2007 *Physics Reports* **452** 155–176 ISSN 0370-1573
[5] Zhou F, Nielson W, Xia Y and Ozoliņš V 2019 *Physical Review B* **100**
[6] Mittal S, Westbroek M J E, King P R and Vvedensky D D 2020 *Eur. J. Phys.* **41** 055401 (*Preprint* `1811.04669`)
[7] Feynman R P 1948 *Rev. Mod. Phys.* **20**(2) 367–387
[8] Perepelitsa D V 2018 *Unpublished Paper*
[9] Hastings W K 1970 *Biometrika* **57** 97–109 ISSN 0006-3444
[10] Gubernatis J E 2005 *Physics of plasmas* **12** 057303
[11] Morningstar C 2007 The Monte Carlo method in quantum field theory *21st Annual Hampton University Graduate Studies Program (HUGS 2006)* (*Preprint* `hep-lat/0702020`)
[12] Joseph A 2020 *Markov Chain Monte Carlo Methods in Quantum Field Theories* (Springer International Publishing)
[13] Binney J and Skinner D 2013 *The physics of quantum mechanics* (Oxford University Press)
[14] Creutz M and Freedman B 1981 *Annals of Physics* **132** 427–462 ISSN 0003-4916
[15] Quenouille M H 1949 *The Annals of Mathematical Statistics* **20** 355 – 375